REGULAR ARTICLE

Increasing the efficiency of postprocessing for turbulent reacting flows

C. Zistl · R. Hilbert · G. Janiga · D. Thévenin

Abstract Turbulent combustion of fossil fuels is nowadays still by far the most important process to cover the worldwide energy needs. Furthermore, turbulent flames are widely used in a wealth of practical applications. Nevertheless, fundamental aspects of turbulent combustion are still poorly understood due to the complexity of the underlying, individual physical processes and due to their complex nonlinear coupling. In order to improve combustion processes, two complementary means are classically used: experimental investigations and numerical simulations. Both lead nowadays to a huge quantity of raw data. In order to extract all useful information from these data, a library containing essential postprocessing methods has been developed: it contains numerous tools to analyze and visualize 2D and 3D flames and flow fields, to investigate geometry and structure of flames both locally and globally, to quantify the interaction between flow fields and flames, and to determine statistics and correlations of all variables that are essential for model development. This library has been coded using scripts implemented into the MATLAB platform. Available tools and illustrative examples are described in this paper in order to demonstrate the interest of this approach.

C. Zistl · R. Hilbert · G. Janiga · D. Thévenin (✉)
Laboratory of Fluid Dynamics and Technical Flows (LSS),
University of Magdeburg "Otto von Guericke",
Universitaetsplatz 2, 39106 Magdeburg, Germany
e-mail: thevenin@ovgu.de

R. Hilbert
LBDR Ingénierie, Paris, France

List of symbols

ϵ	strain rate (s^{-1})
A	area (m^2)
F	variable defining the flame
G_c	Gaussian curvature (m^{-2})
H_c	mean curvature (m^{-1})
k_1, k_2	principal curvatures (m^{-1})
n	normal vector (–)
R_1, R_2	radii of curvature (m)
S	shape factor (–)
t	tangential vector (–)
u	velocity vector (m s^{-1})
$\overline{u_i'^n}$	central moment of order n (m^{n}s^{-n})
W_k	molar mass of species k (kg mol^{-1})
Z	mixture fraction (–)
Z_k	element mass fraction of species k (–)

1 Introduction and problem description

Turbulent reacting flows are essential for a wealth of practical applications (automobile engines, aircraft turbines, domestic boilers, nano-particle production, electricity generation by a power plant burning coal or oil, etc.). Considering the present environmental issues it is essential to understand and improve combustion processes, in order to reduce fuel consumption and pollutant emissions as much as possible. This is indeed a formidable task since turbulent combustion involves many individual, physical processes of high complexity, e.g. chemical kinetics, differential molecular diffusion, radiative heat transfer, phase transition, and of course the turbulent flow itself, which is indeed also an incompletely solved issue. The nonlinear coupling between all these phenomena completely determines the behavior of practical systems. Due to this complex coupling truly predictive numerical models are not

really available at present for realistic installations, although they are of course necessary to improve existing devices and develop new configurations. In order to increase the understanding of the phenomena controlling chemical reactions in a turbulent flow, investigations of simple, model configurations are essential. Two complementary means are used for this purpose: quantitative experimental measurements and accurate numerical simulations. Whenever possible experiments and simulations should be combined, and numerical results should be validated by comparison with experimental data. These investigations can then be used to compute fundamental quantities, for example spatial and temporal correlations between different physical parameters or conditional means of key variables.

There are four main strategies to simulate turbulent reacting flows: the *Reynolds-averaged Navier–Stokes formulation* (RANS: all turbulent scales are modeled) or *Large-Eddy Simulations* (LES: small scales are modeled), possibly combined with *Probability Density Functions* (PDF: mainly employed for turbulent closure); as an alternative, *Direct Numerical Simulations* (DNS: all scales are resolved on the grid) can be used.

RANS are still employed for most industrial applications at present, but require simplified turbulent combustion models and are thus associated with many unsolved issues [1–4]. To some extent, the same remains true for LES of reacting flows due to the need of a subgrid model describing all chemical and diffusive processes taking place below grid resolution, which is a considerable challenge.

The main problem in RANS and LES is to find a closure for the chemical source term. To avoid this problem PDF methods are often used for reacting flows. Transported PDF methods combine an exact treatment of chemical reactions with a closure for turbulence and turbulent transport. A balance equation is resolved for the one-point velocity-composition PDF, wherein the chemical source term is in closed form. When the velocity-composition PDF is known locally, all statistics in that point are known as well. The drawback of one-point methods is that they do not consider gradients. Terms containing such gradients like turbulent scalar fluxes require again a model (like in RANS or LES).

In order to increase the predictive accuracy of numerical simulations, further studies are thus needed to refine the available models or develop alternatives. These studies usually rely either on detailed, quantitative experimental measurements or on DNS computations (sometimes also called "numerical experiments"). The DNS method consists of solving directly the complete, unsteady Navier–Stokes equations. All physical spatial and time scales are resolved accurately so that a turbulence modeling is not necessary any more. When accurate models are also employed for all other physical processes, DNS thus qualify indeed as "numerical experiments", but lead of course to rather high requirements

in computing time and memory. Nevertheless, DNS is the best method with the highest level of accuracy when applicable. DNS results contain all physical information about the turbulent flow as well as all other variables of interest (concentrations, temperature, density…). Due to the resulting extremely lengthy computing time, DNS is not suitable to compute directly practical configurations, but is an optimal method to foster model analysis and development. For this purpose the huge sets of raw data generated by DNS must be postprocessed in an intelligent and efficient manner.

The resulting problems are very similar to those obtained when postprocessing time-resolved experimental measurements (for example from time-resolved particle-image velocimetry [5]), leading to Gigabytes of raw data. Both DNS and experimental investigations produce a huge amount of data, steadily increasing due to the increasing potential of parallel supercomputers and of modern non intrusive, laser-based optical techniques with a high spatial and temporal resolution [6].

For example, the DNS of a 3D hydrogen/air flame presented later in this paper produces typically around 500 MB of raw data *per time-step*. It is obvious that these data have to be postprocessed efficiently in order to extract all the available useful information. Fast, accurate and flexible postprocessing tools are needed in order to maximize the scientific output from such investigations and thus lead to improved models, e.g., for RANS [7] and LES. The key features needed for successful postprocessing tools are that:

- They should allow an easy, standardized, semi-automatic treatment of Gigabytes of raw data, obtained from experimental measurements as well as from DNS.
- They should facilitate the validation procedure, since the same tools will be employed for experimental and numerical results.
- They should be highly flexible in order to satisfy model developers following different lines of thought [8] and in order to be able to cope with non-standardized file formats, containing a highly varying number of variables (two-dimensional vs. three-dimensional data, averaged vs. time-dependent values, single, experimentally measured variable vs. a full set of physical variables obtained from DNS…).

Considering the growing importance of these issues as further documented in a recent review paper [9], and since no such tools are freely (nor even commercially) available yet for turbulent reacting flows, our group has decided a few years ago to start the development of a corresponding library. A first complete version is now available and is the subject of the present paper. In the next section, the general numerical framework is briefly presented. Then, the developed toolbox

is explained in detail, before finally demonstrating its utility for two-dimensional and for three-dimensional DNS results.

The emphasis is clearly set on postprocessing and visualization issues so that the DNS codes employed to compute the corresponding results will not be described at all. The interested reader can refer to [9] and to the listed references of our research group. All possible details concerning numerical methods, algorithmics, physical models or code validation can be found there.

2 Generic numerical environment for postprocessing

The commercial software MATLAB [10] is broadly available in many research groups and contains a wealth of useful, basic bricks for developing an efficient postprocessing library. It is furthermore easily possible to extend MATLAB by writing specific scripts in the native command language similar to C. As a consequence, all the postprocessing routines developed in this project have been written in the form of integrated MATLAB scripts and constitute a specific, add-on toolbox.

The name MATLAB stands for Matrix Laboratory. It is probably the most widespread basic computational tool for engineering sciences in research laboratories and in R&D industrial departments. The main reasons for using MATLAB in the frame of the present project are:

– its comprehensive built-in mathematical library, easily allowing any kind of scalar or matrix computations;
– its powerful basic statistic tools, employed to compute important statistical outputs like moments, correlations or Probability Density Functions (PDFs);
– its extensive graphical and visualization capabilities;
– the possibility of easily extending MATLAB through user-coded scripts.

MATLAB is by default design an interactive programming environment, whose basic data element is a matrix or an array that does not require a priori dimensioning [10]. This allows the solution of many scientific computing problems, especially those relying on two-dimensional matrix or vector formulations in a fraction of the time it would take to write a dedicated program in a scalar non-interactive language. It offers a specific high-level language integrating computation, visualization and further programming functionalities in a unified environment.

In many cases the most suitable way to analyze the wealth of raw data produced by DNS or obtained experimentally is through graphical visualization relying on complex plots. MATLAB provides many basic graphical functions that can be used to create such data plots, like contour plots (for example to visualize scalars directly), vector graphs (use-

ful for example in investigating gradients or in displaying velocity fields) or specific plots for data statistics (such as histograms or scatterplots).

MATLAB also offers several volume visualization techniques allowing representation of 3D data using isosurfaces, vector plots or extracted 2D slices in arbitrary, user-defined directions.

3 Developed postprocessing toolbox

The toolbox developed in this project is intended for postprocessing data produced on a structured, orthogonal grid. Values obtained on another grid type must first be interpolated on such a grid before continuing postprocess. MATLAB offers suitable interpolation schemes for this purpose. The developed toolbox contains presently five different categories of complementary tools:

1. The first group of postprocessing tools is employed for a direct *geometrical analysis* of the raw data in light of turbulent combustion modeling. For this purpose, the essential task is to first

   – define and afterwards locate the flame front.
     Beyond finding the flame front, this group contains also all scripts needed to compute all purely geometrical parameters, e.g.
   – the flame length (in 2D),
   – the flame surface area (in 3D),
   – the flame thickness,
   – the flame curvature and
   – the flame shape factor (in 3D).

2. The second group is dedicated to investigations of the *flame structure*. For this purpose, all the variables computed during any step of the postprocessing can be

   – extracted along the flame front
     (in fact, even along any prescribed isolevel or isosurface of an existing variable). Furthermore, it is possible to compute
   – linear cuts through the flame front
     and any variable of interest can be extracted, integrated or correlated along these cuts. The direction of such a linear cut is constant and normal to the isolevel or isosurface defining the flame front. Finally,
   – nonlinear cuts, following the direction of the steepest gradient of a user-chosen variable,
     can also be computed. Quantities can be extracted along nonlinear cuts similarly as for the previously described linear cuts.

3. Of course, the flame and the turbulent flow field interact with each other. Therefore, the third group of postprocessing tools allows the computation of *important flow variables*, e.g.

   – the vorticity or
   – the strain rate,
     in order to describe and quantify this effect. For a refined analysis of the flow,
   – the streamlines
     can be computed and visualized as well.

4. The fourth group consists of tools allowing a *statistical investigation* of the variables of interest. It is used for example

   – to compute the moments of a distribution,
   – to represent graphically such distributions using for instance histograms, and
   – to determine Probability Density Functions.

5. The fifth and last group contains all the tools needed to investigate and quantify the *properties of turbulent flow* fields. It will output for example

   – turbulent energy distribution,
   – integral scale(s) and
   – velocity fluctuations.

The practical computation of the most important parameters listed previously will be illustrated in Sects. 5 and 6. Table 1 exemplifies typical input and output arguments for the toolbox functions. The presented example is employed to calculate and plot values of a variable extracted along a linear cut through the flame front, defined as an isosurface of a selected variable.

In the next section the main variables considered during postprocessing will be defined. Then, results obtained with the developed toolbox will be illustrated considering DNS results for a non-premixed flame (2D case) as well as a premixed flame (3D case), furthermore using different fuels, in order to demonstrate the flexibility of the procedure.

4 Definitions

Different parameters play a key role in the description and analysis of turbulent combustion. The most important ones are introduced in what follows.

– Mixture fraction
  The mixture fraction Z is the variable which describes the level of mixing between the reactants in a non-premixed flame front. It is a nondimensional variable taking values between 0 for pure oxidizer and 1 for pure fuel. The isole-

Table 1 Example of typical input and output arguments, here to extract and plot a variable along a linear cut perpendicular to the flame front, defined as an isosurface of a given variable

Variable	Function
Input arguments	
X, Y, Z	Vectors defining the rectangular domain
XS,YS,ZS	Coordinates of starting point of the cut
NXS,NYS,NZS	Components of normal vector defining the direction of the linear cut
fdefine	Variable defining the flame front
variable	Variable to be extracted along the cut
level	Isolevel of fdefine defining the flame front
[iso1,iso2]	Isolevels defining boundaries of flame front (optional)
Output arguments	
XMIN, XMAX, YMIN, YMAX, ZMIN, ZMAX	Coordinates of intersection cut-boundaries of flame front
XX1,YY1,ZZ1	Coordinates of the cut
VV1	Values of fdefine along the cut
VV2	Values of variable along the linear cut
VVG	Gradients of fdefine along the cut
plot	Representing variable along cut

vel of Z corresponding to local stoichiometric conditions ($Z = Z_{st}$) is often used to define the flame front. Different definitions of Z can be found in the literature and might be easily implemented in the developed toolbox by the interested user. By default, our library computes the mixture fraction based on chemical elements leading in the case of hydrogen combustion to the formula of Bilger [11]:

$$Z = \frac{\frac{1}{2}Z_H/W_H + (Z_{O,0} - Z_O)/W_O}{\frac{1}{2}Z_{H,0}/W_H + Z_{O,0}/W_O} \quad (1)$$

where Z_H and Z_O are the element mass fractions of the elements H and O and the subscript 0 stands for the initial or boundary conditions on fuel and oxidizer side.
For premixed combustion it is possible to define a progress variable c, which is again a nondimensional variable taking values between 0 (fresh gas mixture) and 1 (burnt gases), and is thus somewhat similar to Z. The progress variable describes the local chemical state between fresh gas and fully reacted mixture.

– Normal vector to the flame front
  It is defined as

$$\mathbf{n} = \frac{\nabla F}{|\nabla F|} \quad \text{along the flame front} \quad (2)$$

where F is the continuous variable employed to define this flame front.

– Strain rate

A flame propagating in a non-uniform flow is subject to strain and curvature effects, which influence local flame structure and behavior and might for instance lead to extinction. The strain rate can be used as a parameter to describe the departure from stable burning conditions. Therefore, it is useful to investigate the strain rate carefully. Along the flame front, the strain rate can be separated into tangential and normal components.

The tangential component is

$$\epsilon_t = \mathbf{t}\mathbf{t} : \nabla\mathbf{u} = t_i t_j \frac{\partial u_i}{\partial x_j} \tag{3}$$

The normal component is

$$\epsilon_n = \mathbf{n}\mathbf{n} : \nabla\mathbf{u} = n_i n_j \frac{\partial u_i}{\partial x_j} \tag{4}$$

where $\mathbf{n}$ and $\mathbf{t}$ are the unit normal and tangential vectors to the flame front. For a 3D flame the tangential part consists of two orthogonal vectors defining a tangential plane to the flame.

– Flame curvature

The curvature is defined as the divergence of the normal vector $\mathbf{n}$ [3], introduced in Eq. (2):

$$\nabla \cdot \mathbf{n} = -\left(\frac{1}{R_1} + \frac{1}{R_2}\right) \tag{5}$$

where $k_1 = 1/R_1$ and $k_2 = 1/R_2$ are the principal curvatures of the flame surface. They measure the highest curvature and the curvature in the perpendicular direction. $G_c = k_1 k_2$ is called the Gaussian curvature and $H_c = (k_1 + k_2)/2$ is called the mean curvature. In differential geometry the Gaussian curvature is classically used to qualify the shape of the surface. The Gaussian curvature is positive for spheres, negative for one-sheet hyperboloids and zero for planes. In turbulent combustion the shape factor is classically used instead.

– Flame shape factor

Following for example [12] the shape factor S is defined as the smallest principal curvature divided by the largest curvature.

$$S = \begin{cases} k_1/k_2 & \text{if } |k_1| < |k_2| \\ k_2/k_1 & \text{otherwise} \end{cases} \tag{6}$$

so that

$$S = \begin{cases} -1 & \text{means the flame has a local saddle point} \\ 0 & \text{means the flame is cylindrically curved} \\ 1 & \text{means the flame is spherically curved} \end{cases}$$

– Probability Density Function f

For a discrete distribution the PDF is the probability that a variable takes a certain value. For continuous distributions the probability that a variable takes a certain value is zero. Therefore, small intervals around that value are considered instead. We thus have to calculate the integral of the variable $f(u_i)$ over the interval of interest. For example, the probability that the variable U_i falls in a particular interval $[ab]$ is given by:

$$P(a \leq U_i \leq b) = \int_a^b f(u_i) du_i \tag{7}$$

– Central moments

Central moments of order n are defined as

$$\overline{u_i'^n} = \int_{-\infty}^{\infty} (u_i - \overline{u_i})^n \cdot f(u_i) du_i \tag{8}$$

where $\overline{u_i}$ is the mean value of the variable and $f(u_i)$ is the PDF describing the distribution.

5 First example: postprocessing of a two-dimensional non-premixed hydrogen flame

The most important tools of the developed MATLAB postprocessing library are now demonstrated by considering first a turbulent, non-premixed, diluted H_2/air flame. The computation relies on a complete reaction scheme, involving 9 chemical species and 37 chemical reactions [13]. The computational domain is 1 cm × 1 cm large, a small but typical size for DNS relying on realistic chemistry. Each direction is associated with 401 grid points in order to reach a sufficient resolution for all intermediate radicals (particularly in the present case for HO_2 and H_2O_2), as well as for the Kolmogorov scale. As usual when dealing with turbulent combustion, the first step is to define and locate the flame front. Since many different possibilities can be found in the literature to define this flame front (a unified definition is missing, and probably unfeasible), different methods have been implemented in the toolbox for this purpose:

– user-defined isolevel or isosurface of a single prescribed variable (this would for example allow to define the flame front as an isolevel of temperature),
– user-defined isolevel or isosurface of a combination of variables (allowing to define the flame front using for example a mixture fraction computed with selected species or elemental mass or mole fractions),
– crest-line of a prescribed variable (for example to define the flame front as the locations of peak heat release).
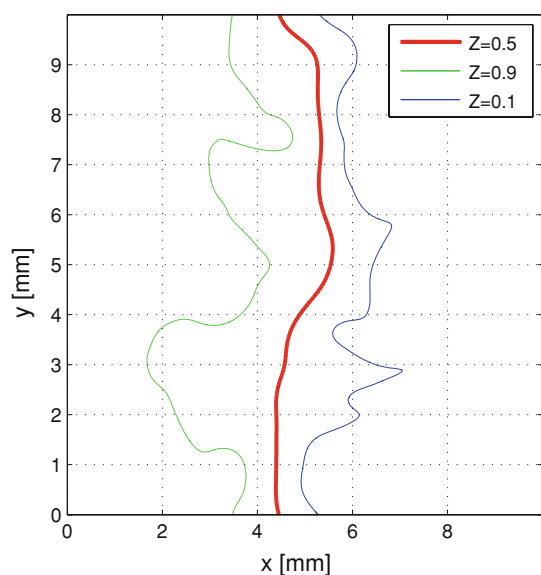
Fig. 1 Extracted flame front (*red line*) based on mixture fraction, together with flame limits (*green line* fuel side, *blue line* oxidizer side)
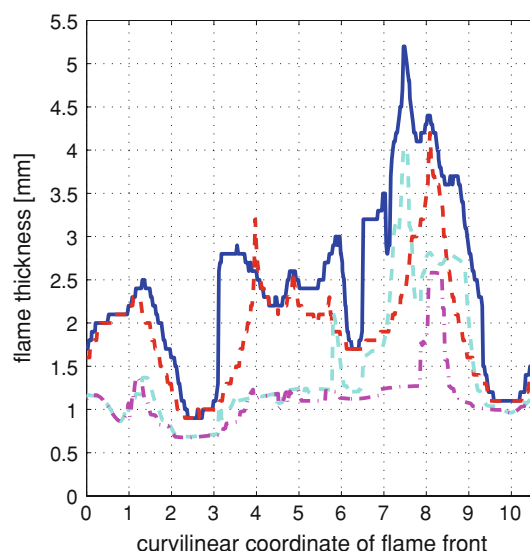

Fig. 2 Flame thickness as a function of the curvilinear flame coordinate (in mm), with 0 at the top of the numerical domain. The flame front is defined as an isolevel of mixture fraction (see Fig. 1). The flame thickness is computed using four possible definitions. *Blue* distance between $Z = 0.1$ and $Z = 0.9$ along linear cuts perpendicular to the flame front. *Red* distance between $Z = 0.1$ and $Z = 0.9$ along nonlinear cuts following mixture fraction gradient. *Cyan* thermal flame thickness using maximal temperature gradient along linear cuts perpendicular to the flame front. *Magenta* thermal flame thickness using maximal temperature gradient along nonlinear cuts following mixture fraction gradient

In the present case, the stoichiometric isolevel of the element-based mixture fraction Z (Eq. 1) is first retained (Fig. 1), since this is quite standard for non-premixed combustion. As an alternative, crest-lines will be considered later on.

After defining and locating the flame, all quantities of interest can be readily computed, and extracted, averaged or correlated along this flame front. To illustrate the procedure, the flame thickness is first computed. Once again, several definitions can be found in the literature that may lead to considerable differences in the analysis. To maximize user-flexibility, it is therefore necessary to implement various definitions within the toolbox. Presently, flame thickness can be computed based:

- on the maximum temperature gradient (thermal flame thickness),
- on considering the real flame extension between user-defined boundaries.

The flame thickness obtained with both definitions is shown in Fig. 2, considering either linear or nonlinear cuts through the flame front. Two curves show the thermal flame thickness, defined as $\Delta T/(\nabla T)_{\mathrm{max}}$, where ΔT is the temperature difference (burnt gas minus fresh gas temperature for a premixed flame, peak minus fresh gas temperature for a nonpremixed configuration) and $(\nabla T)_{\mathrm{max}}$ is the maximum temperature gradient along the local cut through the flame front. The two other curves are obtained when specifying that the flame extends between $Z = 0.1$ on the oxidizer side up to $Z = 0.9$ on the fuel side (second definition), computed along linear cuts (perpendicular to the flame front) or nonlinear cuts (following the steepest gradient of Z). In this

last case, the length of the extracted line is determined by summing up the length of the individual, straight segments employed for discretizing it, with a discretization step given by the original DNS grid. The four different definitions lead to minimum values of 0.7–0.9 mm, maximum values varying between 2.6 and 5.2 mm and mean values between 1.1 and 2.5 mm. This demonstrates that users relying on different definitions might observe very large discrepancies.

The previously described computation of the length is used identically by all tools. For example, the flame length determined in this manner when defining the flame as an isolevel of mixture fraction (x-axis in Fig. 2) is 10.67 mm. Defining the flame as a crest-line of temperature (see for example later the x-axis of Fig. 7), the flame length becomes 10.73 mm.

In some cases it might be inadequate to define the flame front by using isolevels or isosurfaces, and it might be more appropriate and/or more interesting to rely on a crest-line (also called ridge and valley line) connecting all local maximum (or minimum) values of a given variable. A relatively complex procedure has been coded in the developed toolbox to extract automatically such crest-lines as described afterwards. For example Fig. 3 represents the crest-line of temperature, which is in the present, low-turbulence case (Reynolds number based on the integral length scale of turbulence equal to 220, with an integral length scale $L = 1.8$ mm and a velocity fluctuation $u' = 1.89$ m/s; all these quantities
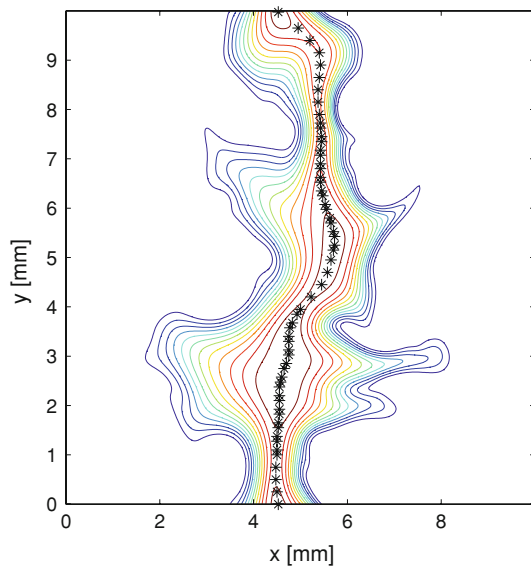
Fig. 3 Crest-line (shown using *black asterisks*) and isolevels of instantaneous temperature (*colored lines*)

Fig. 4 Algorithm to find crest-lines

have been computed using tools belonging to the fifth group of scripts, allowing the analysis of turbulent flow features) visually similar with the mixture fraction isosurface shown in Fig. 1. A quantitative analysis (see later Fig. 7) leads in fact to noticeable differences that would certainly further increase at higher Reynolds numbers. Figure 3 shows also temperature isocontours to demonstrate visually the appropriate computation of the crest-line.

In order to determine the crest-line the program starts in the absolute maximum of the variable (here temperature), scans a square field of predefined size (here with an edge length of 30 cells) around the maximum, searches for the next highest value, jumps to the new maximum and scans a new field around that new maximum in all directions except backwards. The procedure is repeated until either the boundary of the domain is reached or the newest maximum value falls below a prescribed threshold (by default, 50% of the main peak). When the first branch is complete, the program returns to the main maximum, blocks the known branch(es) and searches for further branches.

By default, the program searches for up to three flames and for four branches in each flame. These default values have been found appropriate to analyze all available DNS results up to now. Figs. 4, 5, and 6 explain the procedure for crest-line identification in simple diagrams.

In Fig. 7 the possibility of extracting any predefined quantity along any existing line or surface is illustrated. For this purpose, the local flame temperature is extracted along the crest-line of temperature. This demonstrates that the crest-line is by no way similar to an isolevel of temperature, since variations higher than 300 K are observed along the crest-line.
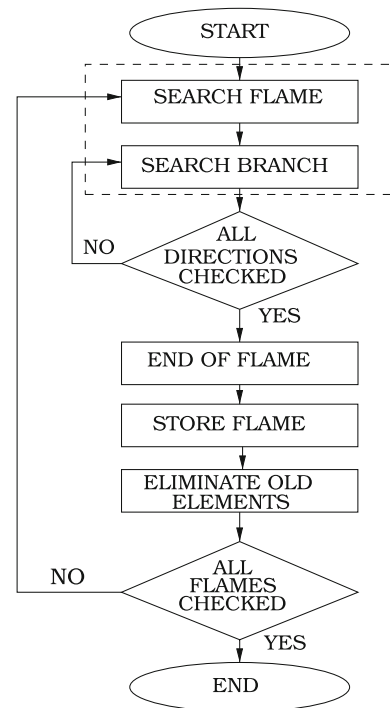
To further investigate the local turbulent flame structure, linear and nonlinear cuts can now be extracted through the flame front. Figure 8 shows as an example a single linear cut, normal to the local, previously defined flame front. Figure 9 shows the local temperature extracted along this cut. The developed toolbox allows prolongation of such cuts up to the computational boundaries of the numerical domain, or as an alternative to stop these cuts when reaching user-defined boundaries. This last procedure has been retained for Figs. 8 and 9, defining again the flame boundaries as $Z = 0.1$ and $Z = 0.9$, as for Fig. 1. Interrupting the extraction in this manner can be used systematically to prevent crossing multiple flame fronts in the case of a highly turbulent, folded flame.

These cuts through the flame are then employed to analyze quantitatively the local flame structure, which is essential to support turbulent combustion modeling [8]. For this purpose the developed toolbox allows to extract along such lines any predefined variable or combination of variables, e.g. temperature, mass fractions, strain rate, heat release, scalar dissipation rate…. As a simple example, Fig. 9 shows the temperature profile extracted along the cut shown in Fig. 8. It is interesting to compare this temperature profile *across the flame* with the temperature profile extracted *along the flame* as shown in Fig. 7 (when defining the flame as a temperature crest-line) as well as in Fig. 10 (when defining the flame as an isolevel of mixture fraction as presented in Fig. 1). Figure 10, furthermore, demonstrates the built-in computation of statistical parameters (mean value, variance, minimum and maxi-
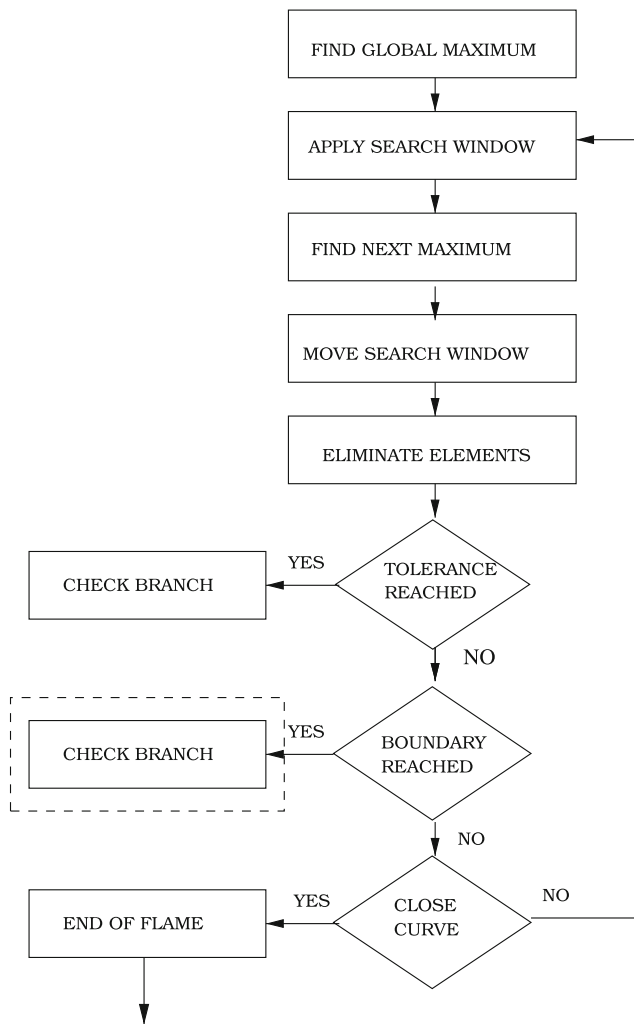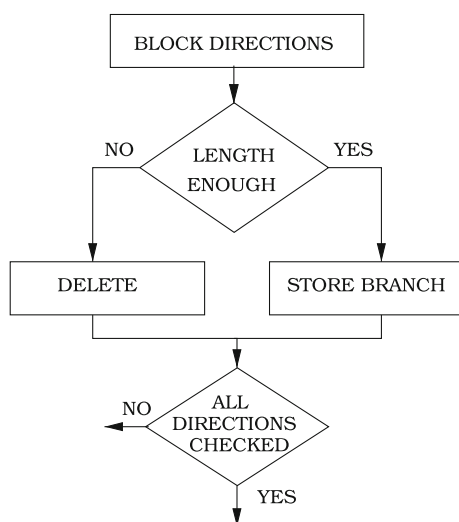
Fig. 5 Algorithm for Search flame and Search Branch

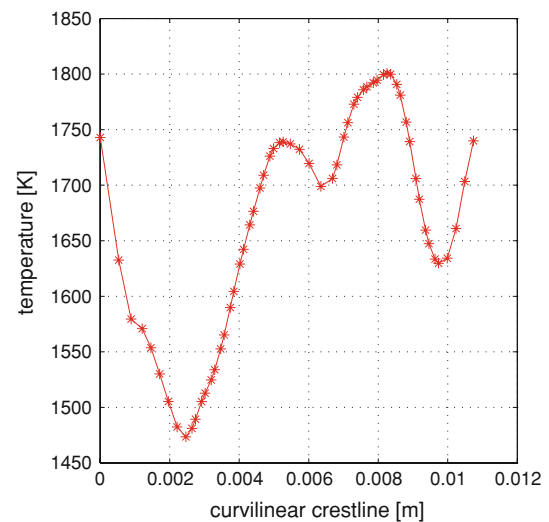

Fig. 6 Algorithm for Check branch

Fig. 7 Local instantaneous temperature (in K) extracted along temperature crest-line (see Fig. 3). Curvilinear coordinate along crest-line in m, with 0 at the top of the numerical domain
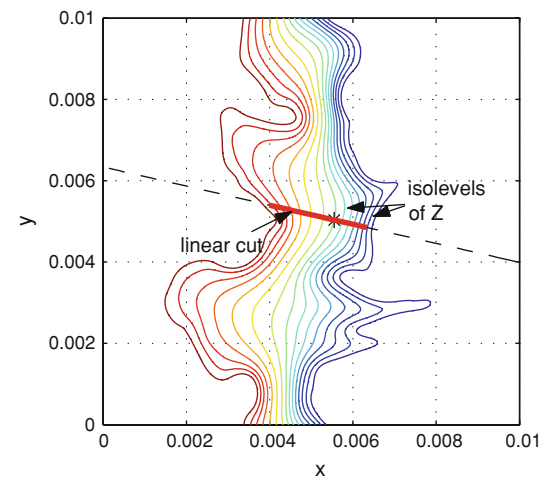

Fig. 8 Local linear cut (*thick red line*) through flame front defined using mixture fraction (see Fig. 1), interrupted at the flame boundaries $Z = 0.1$ and $Z = 0.9$. x and y spatial coordinates in m

mum value) for all predefined variables. A direct comparison of Figs. 7 and 10 reveals that the (user-defined) choice of the definition for the flame front may indeed lead to considerable differences in further quantitative analysis. The minimum temperature along the mixture fraction flame front is for example almost 50 K lower than the corresponding minimum for the flame front built using the temperature crest-line. Finally, Fig. 10 is also interesting as a complementary analysis to Figs. 1 and 3. On these two figures, the isolevels of mixture fraction (Fig. 1) and of temperature (colors in Fig. 3) look very similar to human eyes. One could therefore assume that it would be equivalent to define the flame front as an isolevel of mixture fraction or of temperature. Figure 10 demonstrates that this is indeed far from being true. Along the
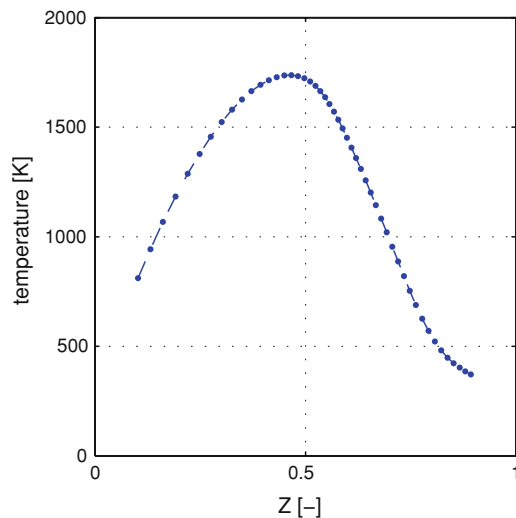
Fig. 9 Local temperature (in K) extracted along the linear cut shown in Fig. 8

Fig. 11 Normal strain rate (in 1/s) along flame front defined using mixture fraction (see Fig. 1). Curvilinear coordinate along flame front in m, with 0 at the top of the numerical domain
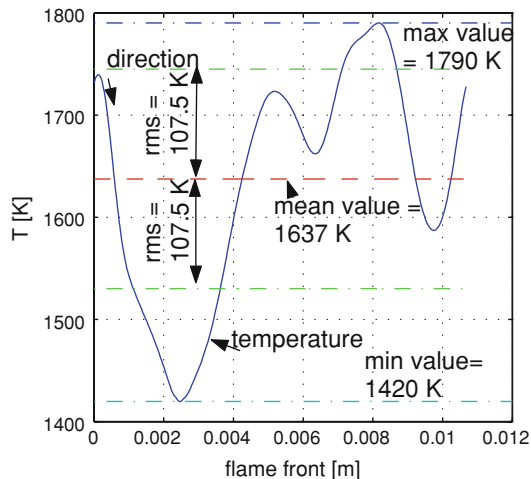

Fig. 10 Temperature (in K) along flame front defined using mixture fraction (see Fig. 1). Curvilinear coordinate along flame front in m, with 0 at the top of the numerical domain

isolevel of mixture fraction used to define the flame front, the local temperature varies by 370 K, and is thus not constant at all. A quantitative postprocessing might thus correct wrong conclusions obtained by a superficial, visual analysis.

In DNS as well as in experiments, the flame and the flow field are directly coupled. Flames can get stretched, thickened or extinguished by turbulence. The quantitative properties of turbulence may be modified by inhomogeneous viscous dissipation and vorticity generation in the flame front. It is therefore essential to be able to compute both the flame and the flow properties. Figure 11 shows for example the local normal strain rate extracted along the flame front. Stretch and strain rates are, together with scalar dissipation, key quantities for modeling purposes [1]. They control in particular extinction
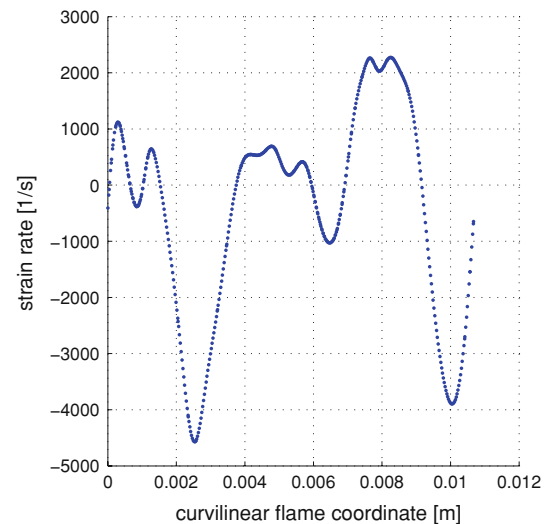
limits. Very large strain rate variations are observed along the flame front, with both compressive and extensive conditions, that will directly influence local burning rates.

It has been already demonstrated in Fig. 10 that standard statistical values (minimum, maximum, mean value and standard deviation) are automatically determined for all defined variables. From a modeling point of view, the statistical analysis of a variable conditioned on another quantity, for example on the mixture fraction Z, is even more interesting since this is a central quantity for most turbulent combustion models [8]. $P(v_1|v_2)dv_1$ is the probability that the first variable (for example the temperature) lies in the range dv_1 around v_1, under the condition that the second variable (for example the mixture fraction) takes on the value v_2. Conditioned moments like mean values and standard deviations are defined in a similar way. The developed toolbox easily allows the computation of such conditional means. Figure 12 shows as an example mean and r.m.s. values for the temperature conditioned on the previously defined mixture fraction Z (Eq. 1). Such results, averaged over time or over several realizations will play a key role for further model testing and improvement.

Histograms, distributions and PDFs can further be easily determined with the developed toolbox. Usually, the correlation between several postprocessed quantities is even more interesting for modeling purposes. Such correlations can be directly computed using the toolbox, and plotted for example as a scatterplot. Figure 13 exemplifies the clear correlation between the local flame thickness and the local strain rate extracted along the flame front defined in Fig. 1. Correlations allow to test and validate modeling hypotheses or to identify unexpected coupling processes.
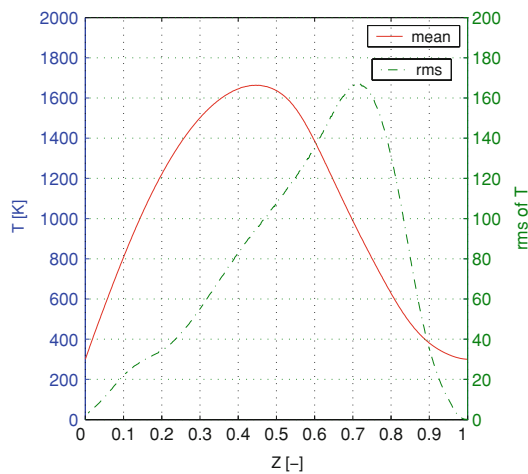
Fig. 12 Mean and r.m.s. values of temperature (in K) conditioned on mixture fraction Z as defined by Eq. (1)

Fig. 14 Streamlines (*blue*) of the two-dimensional turbulent flow interacting with the flame
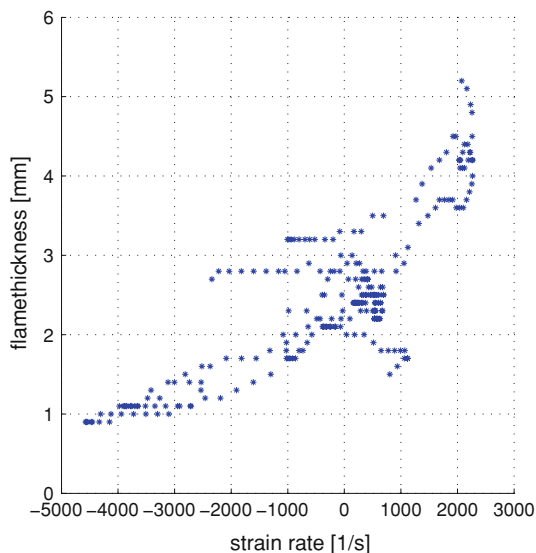

Fig. 13 Correlation between local flame thickness (in mm) and local normal strain rate (in 1/s) along the flame front defined using mixture fraction (see Fig. 1)

6 Second example: postprocessing of a three-dimensional premixed methane flame

In this second case a fully premixed methane-air flame interacts with an initially homogeneous and isotropic turbulent flow field within a three-dimensional computational domain. The length of this domain is 5 mm in each direction, discretized with 101 grid points, leading to one million total grid points. Many aspects of the postprocessing are qualitatively similar to the two-dimensional treatment illustrated in the previous section, so that shorter explanations should be sufficient to comment the proposed figures. Note, however, that *quantitatively* the postprocessing of three-dimensional data is much more complex than in 2D.

In order to get a first visual feeling of flame structure and topology, slices obtained by keeping a constant value for the x, y or z coordinate are easily obtained and might be useful for probing the 3D-field. Therefore, Fig. 15 shows a horizontal ($z = $ constant) slice through the middle of the domain. Along such slices, all the tools previously introduced for two-dimensional results might be readily employed. In Fig. 15, three isolevels of one combustion product (CO_2) mass fraction are shown. The flame front is defined for this premixed case as the isolevel $Y(CO_2) = 0.03$, where Y denotes the mass fraction. This definition results from a previous analysis dedicated to the present configuration [14]. The boundaries of the flame are defined between $Y(CO_2) = 0.007$ (fresh gas side) and $Y(CO_2) = 0.06$ (burnt gas side), see Fig. 15. Figure 15 shows furthermore two-dimensional streamlines within the same plane.

After getting a first feeling thanks to such two-dimensional slices, the next logical step is to switch to real, three-dimensional visualizations and analysis. It is once again

Last but not least, the postprocessing toolbox can be employed to analyze the main features of the turbulent flow. Figure 14 shows, as an example, the streamlines associated with the two-dimensional velocity field interacting with the flame. Large vortical structures appear clearly and can be analyzed to understand flame displacement. The flame region in the center of the domain is associated with high dissipation rates (high viscosity), leading to a damping of vorticity.
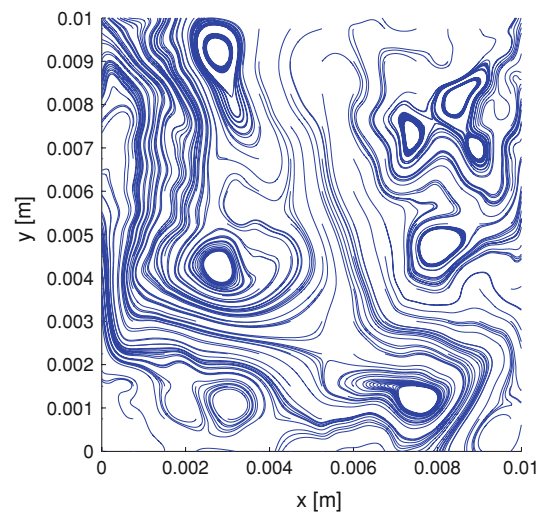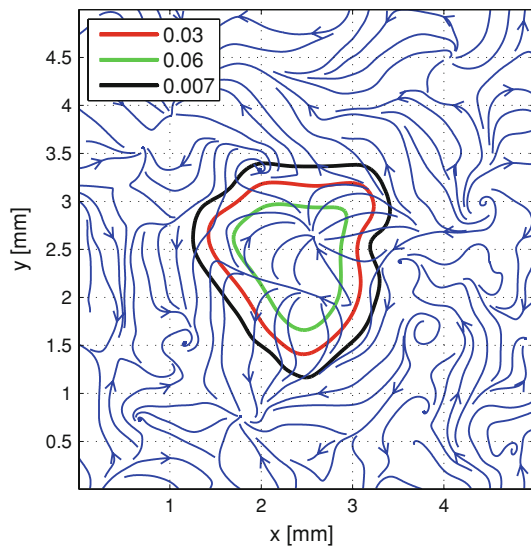
Fig. 15 Streamlines (*blue*) of the turbulent flow interacting with the flame shown along a horizontal slice through the middle of the computational box. On the same figure three isolevels of CO_2 mass fraction are shown (*red* flame front, *black* fresh gas limit, *green* burnt gas limit

Fig. 16 Flame front for the three-dimensional premixed methane flame, defined as an isosurface of CO_2 mass fraction. All spatial coordinates in mm

recommended to start by defining the flame front in 3D. Figure 16 shows this flame front, defined as the isosurface $Y(CO_2) = 0.03$, as explained previously. After locating the flame front, the local flame structure can readily be analyzed in a quantitative manner. For this analysis, all the features described previously for the two-dimensional cases are still available. The developed toolbox allows once again the computation and graphical representation of any predefined variable of interest or combinations of such variables, along any predefined isosurface. As an example, Fig. 17 shows the normal component of the strain rate along the flame surface. The distribution of this normal strain rate is shown as a histogram in Fig. 18, allowing a better quantification of the huge strain rate variations observed in this configuration.

Considering the extremely high cost of three-dimensional DNS computations of reacting flows with a realistic chemistry, two-dimensional simulations are still a very valuable alternative for all configurations where three-dimensional effects are small [3]. In order to find out whether the flame front can be considered as mostly cylindrical (and thus dominated by two-dimensional features) or spherical (and therefore fully three-dimensional), it is necessary to determine quantitatively the curvature of the flame surface. For this purpose, the principal curvatures, k_1 and k_2, are computed using the developed toolbox along with the shape factor S (Eq. 6) stating if the local structure is mostly cylindrical or spherical (see Fig. 19).

The implemented procedure has been successfully validated using perfect spheres and cylinders of known radius. Such computations exemplify quantities that only make sense for three-dimensional computations and have been added
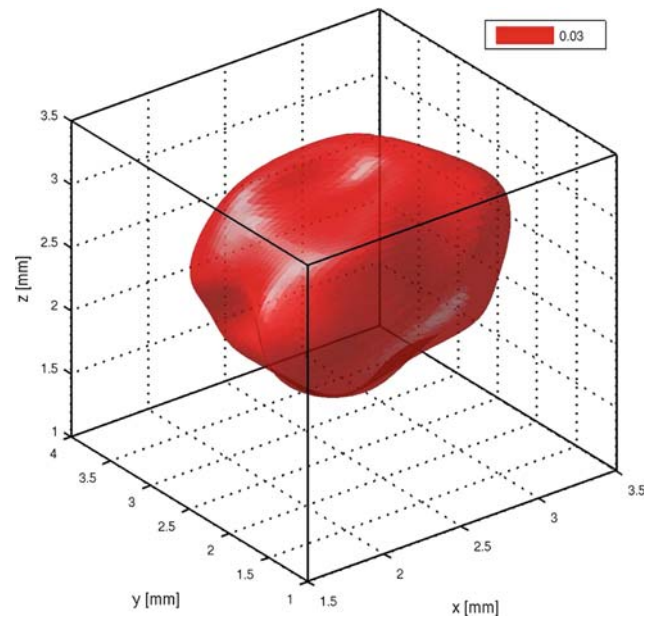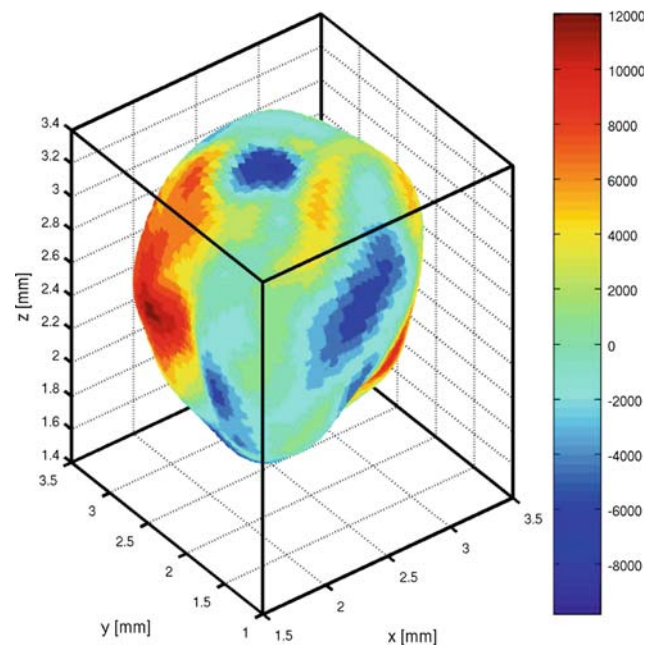

Fig. 17 Normal strain rate (in 1/s) along flame front (see Fig. 16). All spatial coordinates in mm

recently to the postprocessing toolbox. Figure 19 demonstrates in particular that the investigated turbulent flame is dominated locally by cylindrical properties, a fact already observed in previous studies [3]. Therefore, two-dimensional DNS computations of such flames might indeed deliver useful information, at least for the low Reynolds numbers considered in the present cases.
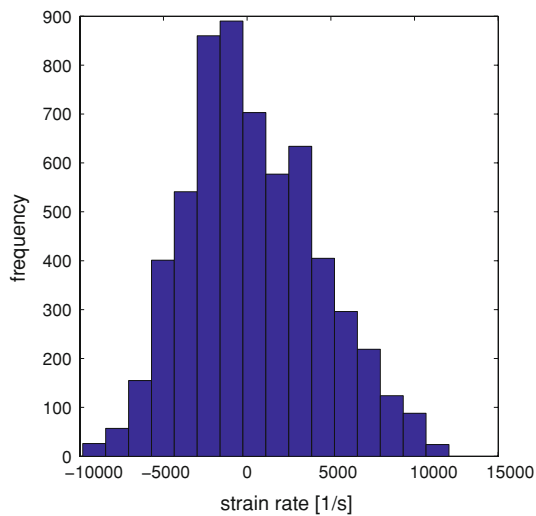
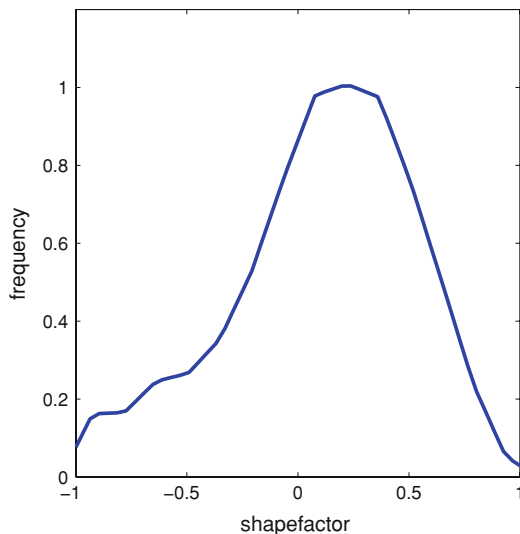**Fig. 18** Histogram showing the distribution of normal strain rate (in 1/s) along flame front (see Fig. 16)

Fig. 20 Linear cut (*bold red segment*) through the flame front (see Fig. 16). Three different isosurfaces of CO_2 mass fraction are shown in this figure. All spatial coordinates in mm

Fig. 19 Distribution of shape factor along flame front shown in Fig. 16

Fig. 21 Distribution of the x-component of velocity (*vertical bars* and *blue line*, in m/s), by comparison with a Gaussian distribution associated to the same first moments (*red line*)

Figure 20 shows a linear cut through the flame front using the flame definition and the flame boundaries mentioned previously. The starting point of the linear cut is taken here on the isosurface defining the flame front. This figure, compared to Fig. 8, illustrates clearly the additional complexity associated with three-dimensional data.

All statistical tools available in two dimensions can be directly used also in 3D. For example, the moments of any extracted distribution can be computed automatically, allowing comparisons with standard distributions when appropriate. To illustrate this point, the resulting statistics for the x-component of the present velocity field are presented in Fig. 21 as a PDF histogram. Computing the first moments of this distribution and using these values to generate a Gaussian
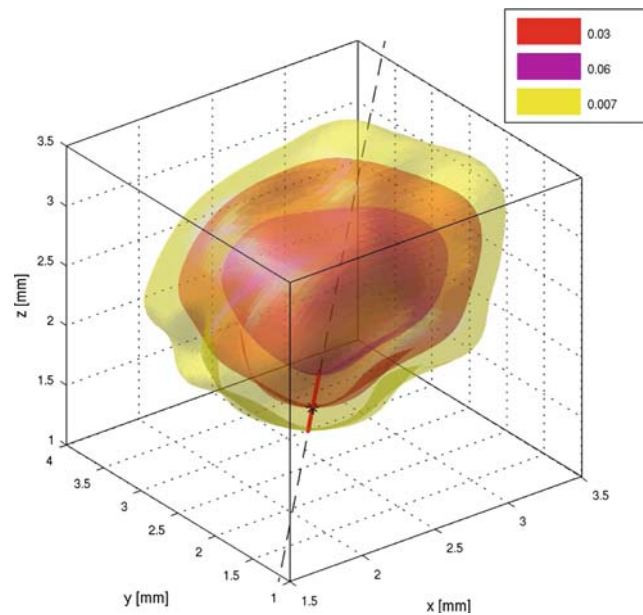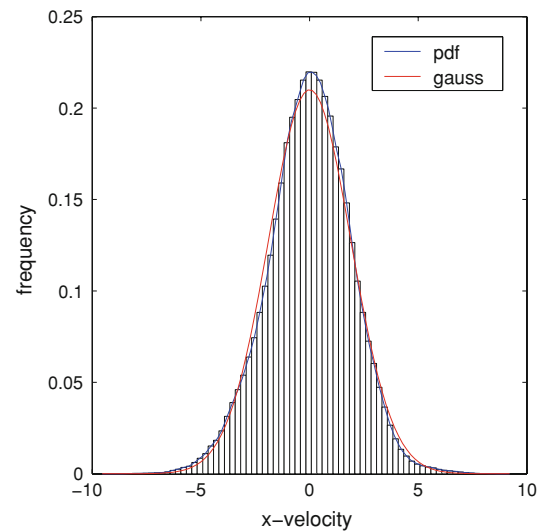
distribution [15], a comparison can be easily obtained, demonstrating the nearly Gaussian nature of the turbulent velocity field in the present configuration (low turbulence level, early stage of flame development).

7 Conclusions and perspectives

In this paper a large postprocessing toolbox has been presented. It is developed on top of MATLAB to analyze efficiently

and in a quantitative manner large data sets obtained by DNS or by experimental measurements of turbulent reacting flows. A wealth of complementary features is already available in this toolbox and have been illustrated considering both two-dimensional and three-dimensional configurations, non-premixed and premixed flames and different fuels (hydrogen and methane). This demonstrates the high flexibility of the developed tool, since the user does not need to modify anything in order to be able to investigate these various problems. Many computed quantities have been shown graphically, but many more can of course be computed and visualized, which could not be shown here due to lack of space.

The developments are now completely finished for two-dimensional analyses. Further scripts are presently implemented in the three-dimensional version, particularly regarding data filtering, needed to analyze subgrid-scale issues and support progress in LES modeling of turbulent flames. It is expected that the toolbox will be fully completed at the beginning of 2008. A free, Internet-based distribution will then be organized.

References

1. Peters, N.: Turbulent Combustion. Cambridge University Press (2000)
2. Warnatz, J., Maas, U., Dibble, R.W.: Combustion, 3rd edn. Springer, Berlin (2001)
3. Poinsot, T., Veynante, D.: Theoretical and Numerical Combustion. R. T. Edwards Publishing, USA (2001)
4. Fox, R.O.: Computational Models for Turbulent Reacting Flows. Cambridge University Press, London (2003)
5. Krause, N., Zähringer, K., Pap, E.: Time-resolved particle imaging velocimetry for the investigation of rotating stall in a radial pump. Exp. Fluids **39**, 192–201 (2005)
6. Konle, M., Winkler, A., Kiesewetter, F., Wäsle, J., Sattelmayer, T.: CIVB flashback analysis with simultaneous and time resolved PIV-LIF measurements. In 13th International Symposium on Applications of Laser Techniques to Fluid Mechanics. Lisbon, Portugal (2006)
7. Tap, F., Hilbert, R., Thévenin, D., Veynante, D.: A generalized flame surface density modelling approach for the auto-ignition of a turbulent non-premixed system. Combust. Theory Model **8**, 165–193 (2004)
8. Veynante, D., Vervisch, L.: Turbulent combustion modeling. Prog. Energy Combust. Sci. **28**(3), 193–266 (2002)
9. Hilbert, R., Tap, F., El-Rabii, H., Thévenin, D.: Impact of detailed chemistry and transport models on turbulent combustion simulations. Prog. Energy Combust. Sci. **30**, 61–117 (2004)
10. Mathworks (2005). Using Matlab 7. The MathWorks Inc. Natick, MA, 2005
11. Bilger, R.W.: The structure of turbulent nonpremixed flames. In: Twenty-second Symposium (International) on Combustion, pp. 475–488. The Combustion Institute, Pittsburgh (1988)
12. Rutland, C.J., Trouvé, A.: Direct simulations of premixed turbulent flames with nonunity Lewis numbers. Combust. Flame **94**, 41–57 (1993)
13. Maas, U., Warnatz, J.: Ignition processes in carbon-monoxide-hydrogen-oxygen mixtures. In: Twenty-second Symposium (International) on Combustion, pp. 1091–1098. The Combustion Institute, Pittsburgh (1988)
14. Thévenin, D., Gicquel, O., de Charentenay, J., Hilbert, R., Veynante, D.: Two- versus three-dimensional direct simulations of turbulent methane flame kernels using realistic chemistry. Proc. Combust. Inst. **29**, 2031–2039 (2002)
15. John, V., Angelov, I., Öncül, A., Thévenin, D.: Techniques for the reconstruction of a distribution from a finite number of its moments. Chem. Eng. Sci. **62**, 2890–2904 (2007)